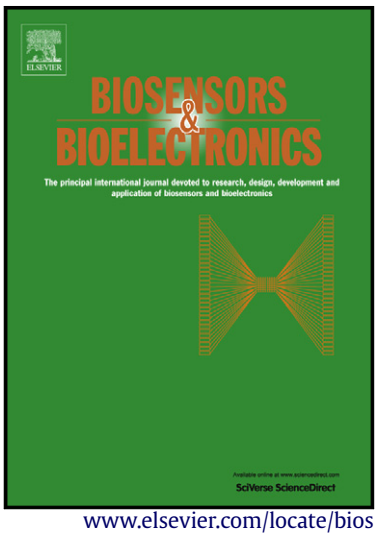

www.elsevier.com/locate/bios

Amperometric detection of catechol using tyrosinase modified electrodes enhanced by the layer-by-layer assembly of gold nanocubes and polyelectrolytes

Md. Nurul Karim, Ji Eun Lee, Hye Jin Lee

PII: S0956-5663(14)00344-3
DOI: http://dx.doi.org/10.1016/j.bios.2014.05.011
Reference: BIOS6773

To appear in: *Biosensors and Bioelectronics*

Received date: 2 February 2014
Revised date: 3 May 2014
Accepted date: 5 May 2014

Cite this article as: Md. Nurul Karim, Ji Eun Lee, Hye Jin Lee, Amperometric detection of catechol using tyrosinase modified electrodes enhanced by the layer-by-layer assembly of gold nanocubes and polyelectrolytes, *Biosensors and Bioelectronics,* http://dx.doi.org/10.1016/j.bios.2014.05.011

Amperometric detection of catechol using tyrosinase modified electrodes enhanced by the layer-by-layer assembly of gold nanocubes and polyelectrolytes

Md. Nurul Karim[a], Ji Eun Lee[b] and Hye Jin Lee[a]*

[a]*Department of Chemistry and Green-Nano Materials Research Center, Kyungpook National University, 1370 Sankyuk-dong, Buk-gu, Daegu, 702-701, Republic of Korea*

[b]*Center for Theragnosis, Biomedical Research Institute, Korea Institute of Science and Technology, Hwarangno 14-gil 5, Seongbuk-gu, Seoul 136-791, Republic of Korea*

**E-mail address: hyejinlee@knu.ac.kr and Phone number: +82 (053) 950-5336*

Abstract

A novel amperometric biosensor for catechol was developed using the layer-by-layer (LbL) self-assembly of positively charged hexadecyltrimethylammonium stabilized gold nanocubes (AuNCs), negatively charged poly(sodium 4-styrenesulfonate) and tyrosinase on a screen printed carbon electrode (SPCE). A carboxylic acid terminated alkanethiol assembled on electrochemically deposited Au nanoparticles on a SPCE was used as a platform for LbL assembly. Each SPCE sensor surface was terminated with tyrosinase and the electrocatalytic response due to the tyrosinase reaction with catechol was measured using cyclic voltammetry and square wave voltammetry (SWV). The effect of introducing AuNCs into the LbL assembly to further enhance the catechol detection performance was then investigated by comparing the SWV results to those from biosensors created using both the tyrosinase modified LbL assembly in the absence of NCs and the covalent attachment of tyrosinase. A wide dynamic range from 10 nM to 80 μM of catechol with an excellent sensitivity of 13.72 A/M and a detection limit of 0.4 nM were both achieved alongside a good selectivity and reproducibility for the AuNC-modified electrodes. As a demonstration, the optimized biosensor design was applied to determine catechol concentrations in tea samples.

Keywords

Amperometric biosensor; Catechol; Gold nanocubes; Tyrosinase; Layer-by-Layer; Screen printed carbon electrode

1. Introduction

Catechol (1,2-dihydroxybenzene), a natural compound present in teas, vegetables, tobaccos and traditional medicines is known to be harmful to human health as well as animals (Figueiredo et al., 2007). It is thus of great interest to develop a rapid, sensitive and convenient method for the determination of catechol in environmental, food and biological samples. The most commonly used analytical methods for catechol include spectrometry (Figueiredo et al., 2007), gas chromatography-mass spectrometry (Moldoveanu and Kiser, 2007) and high-performance liquid chromatography (Cui et al., 1999). These methods offer excellent accuracy and precision but suffer from complicated sample pretreatment, large time-consumption and inconvenient on-site monitoring. Electrochemical biosensors are an excellent alternative due to their cost-effective fabrication, high sensitivity and easy handling in field applications (Lv et al., 2010). The selectivity of electrochemical sensors for the sensing of catechol can be greatly enhanced by the use of enzyme modification (Sarma et al., 2009). One of the most commonly used enzymes for catechol sensing is tyrosinase (Tyr) which selectively catalyzes the oxidation of catechol to *o*-quinone in the presence of molecular oxygen followed by the electrochemical reduction of liberated *o*-quinone species. Tyrosinase phosphate-doped polypyrrole modified electrodes and tyrosinase modified multi-walled carbon nanotubes were recently reported for catechol sensing with a detection limit of ~1 μM (Apetrei et al., 2011; Vicentini et al., 2013). Enzymes can be immobilized on electrode surfaces via various strategies including encapsulation in a sol-gel matrix (Singh et al., 2013), covalent coupling chemistry (Karim and Lee, 2013) in addition to facile layer-by-layer (LbL) assembly processes utilizing the electrostatic interaction of oppositely charged species (Decher, 1997).

In this paper, we demonstrate a novel and highly reproducible amperometric biosensor design based on the LbL assembly of AuNCs and polyelectrolytes in conjunction with tyrosinase for the enhanced sensitive and selective detection of catechol. The incorporation of metallic nanoparticles into electrode materials has been previously investigated to enhance biosensor sensitivities for phenolic compounds (Campbell and Compton, 2010; Karim and Lee, 2013; Luo et al., 2006; Song et al., 2011). For example, a graphene oxide-AuNP electrochemical sensor also modified with tyrosinase has been employed to detect catechol down to 24 nM (Song et al., 2011). In addition, the combined use of gold nanoparticles (AuNPs), polyelectrolytes and attached enzymes has been reported on carbon electrode surfaces (Fang et al., 2010). However, LbL assembly utilizing gold nanocubes (AuNCs) and combining with enzyme attachment on an electrode surface has not yet been reported. In our approach, a negatively charged alkanethiol was assembled onto AuNPs deposited on a screen printed carbon electrode (SPCE) followed by the sequential electrostatic adsorption of positively charged hexadecyltrimethylammonium bromide (CTAB) stabilized AuNCs and negatively charged poly(sodium 4-styrenesulfonate) (PSS) electrolytes. Tyrosinase was then electrostatically immobilized onto the positively charged CTAB-AuNC layer of the LbL electrode (see Fig. 1a). The performance of the catechol biosensor including sensitivity, reproducibility and stability was evaluated using cyclic voltammetry and square wave voltammetry. This included optimizing design parameters such as the number of AuNC and PSS LbL layers as well as comparing with LbL sensor surfaces with no AuNC's present and also where tyrosinase is instead covalently attached directly onto AuNPs deposited on a SPCE. As a demonstration, the AuNC incorporated biosensor was employed to

analyze catechol concentrations in commercial tea samples with the data also validated by UV-vis spectroscopy measurements.

2. Experimental Section

Additional details beyond the points discussed below are provided in the Supporting Information.

2.1. Preparation of Au nanocube enhanced biosensor by LbL assembly on SPCE

The LbL assembly process of AuNCs with an average size of 45 nm (see Fig. S1) and PSS on AuNP deposited SPCE followed by the adsorption of tyrosinase is illustrated in Fig. 1a. Briefly, AuNPs were first deposited onto the SPCE surface using a method described previously (Karim and Lee, 2013) followed by immersing the electrode in 20 mM MPA solution (75/25%, v/v, absolute ethanol/water) for 15 h at room temperature. After rinsing the electrode with ethanol and water followed by drying with a N_2 stream, the LbL process was performed by alternately dipping the MPA modified SPCE in AuNC/CTAB and PSS solutions for a 30-min period. After rinsing with water and drying under N_2, the final AuNC layer was then exposed to a 10 µL aliquot of tyrosinase solution for 6 h at 4 ^{o}C. Prior to any electrochemical measurements, each tyrosinase modified SPCE was washed with 0.1 M phosphate buffer solution (pH 7.0) and stored at 4 ^{o}C.

2.2. Electrochemical measurements

A computer controlled potentiostat (Autolab PGSTAT128N, Ecochemie) was used for all electrochemical measurements. Custom made SPCEs were composed of a carbon working electrode with a geometric working area of 28 mm^2, a Ag/AgCl reference and a carbon counter electrode. All electrochemical measurements were performed at room temperature with 0.1 M phosphate buffer solution (pH 7.0) unless otherwise specified.

3. Results and discussion

3.1. Characterization of Tyr-AuNC-(PSS-AuNC)$_2$ -MPA-AuNP modified biosensors for catechol

The surface morphology alongside the size distribution and layer thickness of gold nanoparticles and nanocubes assembled on the SPCE were characterized using scanning electron microscopy (SEM) and atomic force microscopy (AFM) (see Fig. 1b-c and Fig. S2). The SEM data revealed that the bare SPCE has a typical surface roughness associated with carbon paste (Lee et al., 2007) and that the electrochemically deposited AuNPs have an average diameter of 120 ± 5 nm and were uniformly distributed. Following LbL assembly, densely packed layers of AuNCs with an average size of 135 ± 5 nm were present for a AuNC-(PSS-AuNC)$_2$-MPA-AuNP modified SPCE (see Fig. 1b). From cross-sectional line profiles of AFM data, the thickness of a AuNC layer was estimated as ~200 nm (see Fig. 1c) from the surface of AuNP deposited SPCE. The significant differences in morphologies and thicknesses between the AuNP-SPCE and multilayered AuNC-PSS modified SPCE confirms the presence of AuNCs on the electrode and also that the LbL process can be efficiently used to modify the electrode surface with AuNCs.

The catechol sensing performance of the NC assembled electrode sensor design was initially assessed using cyclic voltammetry. Fig. 1d shows representative cyclic voltammograms for different catechol concentrations when using the Tyr-AuNC-(PSS-AuNC)$_2$-MPA-AuNP modified SPCE. In the absence of catechol (i), the electrode showed only a small background current. As the catechol concentration increased, a reduction peak with a sigmoidal-shaped current response at -50 mV (vs. Ag/AgCl) increased due to the electrochemical reduction of *o*-quinone liberated from the catalytic surface reaction between tyrosinase and catechol. A linear relationship between the cathodic peak current and catechol concentration was found over a concentration range between 0.8 µM and 80 µM with a sensitivity of 0.04 A/M. Three different chips were repeatedly tested at each catechol concentration and the averaged values are presented in Fig. S3. This confirms that tyrosinase retains its bioactivity following surface immobilization onto the LbL film. It was also discovered that increasing the number of repeat (PSS-AuNC) layers improved the sensing performance. However, when the number of AuNC layers exceeded three, a drop in the current response was observed that is probably due to limited mass transport of redox species to the electrode surface (see Fig. S4). Hence, three AuNC layers were used for all subsequent experiments reported here.

3.2. Square wave voltammetric determination of catechol and real tea sample analysis

Further enhancement in the sensitivity of the catechol sensor was achieved using square wave voltammetry (SWV). Experimental parameters including pH of the phosphate buffer solution, electrochemical cell temperature and enzyme loading concentration used when immobilizing

tyrosinase onto AuNC assembled electrode surfaces were first optimized as pH 7.0, 35 ^{o}C and 29.7 µg mL^{-1}, respectively (see Figs. S5-S7). Note that the biosensor response was highest at 35 ^{o}C, however, all subsequent measurements were performed at 25 ^{o}C (which shows 20% less in the current response) for practical reasons including the long-term stability of the sensor and performing future measurements in portable devices. Fig. 2a shows the SWV responses of a Tyr-AuNC-(PSS-AuNC)$_2$-MPA-AuNP-SPCE for different concentrations of catechol ranging from 0.4 nM to 170 µM. A peak at -100 mV (vs. Ag/AgCl) associated with the reduction of *o*-quinone to catechol increased with respect to catechol concentration. Two different linear response regions were established over the catechol concentration ranges studied; from 10 to 100 nM, a slope of 13.72 A/M was obtained (Fig. 3 inset), which is about 30 times more sensitive than the 0.1 to 80 µM range where a slope of 0.39 A/M was measured (Fig. 3a). An excellent detection limit of 0.4 nM catechol was evaluated according to the $3s_b/m$ criteria, where s_b is the standard deviation of the blank response and m is the corresponding slope from the calibration curve. This is comparable to previously reported tyrosinase-nanoparticle modified biosensors (Ozoner et al., 2010) and also about 1000 times better than that of using a tyrosinase modified electrode in the absence of AuNCs (see Fig. 3c).

In order to further assess the effect of nanocubes on the enhancement of the sensor performance, two different biosensing configurations in the absence of nanocubes were fabricated. These were: (i) Tyr-AuNP-SPCE where the enzyme was covalently immobilized onto the electrodeposited NP's using EDC/NHS linking chemistry; and (ii) LbL assembly of CTAB and PSS layers on the MPA modified electrodeposited AuNP's (Tyr-CTAB^{+}-(PSS^{-}-CTAB^{+})$_2$-MPA-AuNP-SPCE). Figs.

2b-c show SW voltammograms for catechol using Tyr-AuNP-SPCE and Tyr-CTAB^{+}-(PSS^{-}-CTAB^{+})$_2$-MPA-AuNP-SPCE, respectively. All SWV current values were normalized with respect to the background current and reported as an average of three separate determinations using three different chips for each single catechol concentration. The peak responses at -20 and -100 mV (vs. Ag/AgCl) obtained for Tyr-AuNP-SPCE and Tyr-CTAB^{+}-(PSS^{-}-CTAB^{+})$_2$-MPA-AuNP-SPCE, respectively are associated with the reduction of *o*-quinone to catechol. The -80 mV shift in the peak potential between these two electrodes follows the same trend for the Tyr-AuNC-(PSS-AuNC)$_2$-MPA-AuNP modified SPCE described above where there is a difference in the number of polyelectrolyte multilayers (Hodak et al., 1997).

Comparing the analytical performances of the different surface layer configurations (see Table S1) revealed that the AuNC incorporated biosensor showed the widest dynamic range of 10 nM to 80 µM while the Tyr-CTAB^{+}-(PSS^{-}-CTAB^{+})$_2$-MPA-AuNP-SPCE had the lowest dynamic range of 2.0 µM to 70 µM. In addition, the incorporation of AuNCs improved the sensitivity ~5 fold compared to that of the Tyr-AuNP-SPCE. It is interesting to note that while the sensitivity of the AuNC assembled sensors was similar to that of the LbL assembled biosensor without NCs, the detection limit was dramatically enhanced (about 1000 times). A possible explanation for the large improvement when incorporating AuNC's into the multilayer structure may be that the effective electroactive surface area of the electrode has been increased while the film porosity ensures good mass transport properties at the electrode surface (Liu et al., 2006). The effective electroactive surface area of each biosensor configuration was estimated using voltammetric measurements with a well-known redox probe, $Fe(CN)_6^{4-/3-}$ (see Fig. S8 and Table S2 alongside

further details in the Supporting Information). This measurement is only a rough estimate, however, each electrode surface configuration can be compared relatively. The results showed that the electroactive area of the AuNP-SPCE electrode was ~2 times higher than the carbon only surface. The effective area further increases with the introduction of AuNC layers with the AuNC-(PSS-AuNC)$_2$-MPA-AuNP-SPCE configuration about two times larger than that of AuNP-SPCE.

Chip-to-chip variations were investigated by measuring the SWV responses for a fixed concentration of 5.0 µM catechol with eight independently prepared Tyr-AuNC-(PSS-AuNC)$_2$-MPA-AuNP-SPCE biosensors and the relative standard deviation (RSD) value was 5.6% (see Fig. S9), which is considerably better than for Tyr-AuNP-SPCE (10.7%). The long-term stability of our AuNC enhanced biosensor was also studied via measuring SWV responses for 5.0 µM catechol three times per day for 16 days while the sensor was continuously stored in buffer solution. A RSD value of 6.2% was obtained and the sensor retained 83% of its initial activity after 9 days (see Fig. S10). The selectivity for catechol in the presence of several common interfering divalent cations, anions and organic molecules was also studied (see Fig. S11 and Table S3). Of the various species studied, strong interference effects were observed for excess Cu^{2+} ions, hydroquinone and dopamine when they were present at 100-fold greater concentrations compared to catechol.

As a final demonstration, the Tyr-AuNC-(PSS-AuNC)$_2$-MPA-AuNP-SPCE was used for the determination of catechol in five different bottled green and black tea drinks diluted in buffer

solution. The SWV results are summarized in Fig. S12 and Table S4 indicates that most tea drinks contain catechol concentrations of 9-16 mM and this was also validated by analyzing the same tea samples utilizing UV-visible spectroscopic methods (see Figs. S13-14). The good agreement in both analyses indicates that the AuNC LbL electrode biosensors can be used as a reliable and effective analytical tool for catechol determination in real samples.

4. Conclusion

In summary, a highly sensitive biosensor for catechol offering a detection limit of 0.4 nM has been developed based on the systematic assembly of multilayer films composed of AuNC's, PSS and tyrosinase on SPCEs and the biosensors were also applied to the rapid and successful analysis of catechol concentrations in commercial tea samples. One of the remaining challenges is to maintain the long term stability of the sensor at room temperature since the performance is dependent on a surface-attached enzyme layer in addition to improving the selectivity for organic molecules by incorporating different enzymes. Further improvements in expanding the LbL biosensor's applicability towards food, environmental and biological science research and industry are underway.

Acknowledgement

This research was supported by Basic Science Research Program through the National Research Foundation of Korea (NRF) funded by the Ministry of Science, ICT and Future Planning (NRF-2013R1A2A2A03068833) and the Intramural Research Program of KIST.

References

Apetrei, C., Rodriguez-Mendez, M.L., Saja, J.A.D., 2011. Electrochim. Acta 56, 8919-8925.

Campbell, F.W., Compton, R.G., 2010. Anal. Bioanal. Chem. 396, 241-259.

Cui, H., He, C., Zhao, G., 1999. J. Chromatogr. A 855, 171-179.

Decher, G., 1997. Science 277, 1232–1237.

Fang, Y., Guo, S., Zhu, C., Zhai, Y., Wang, E., 2010. Langmuir 26, 11277-11282.

Figueiredo, E.C., Tarley, C.R.T., Kubota, L.T., Rath, S., Arruda, M.A.Z., 2007. Microchem. J. 85, 290-296.

Hodak, J., Etchenique, R., Calvo, E.J., 1997. Langmuir 13, 2708-2716.

Karim, M.N., Lee, H.J., 2013. Talanta 116, 991-996.

Lee, C.-H., Wang, S.-C., Yuan, C.-J., Wen, M.-F., Chang, K.-S., 2007. Biosens. Bioelectron. 22, 877-884.

Liu, B.A., Wei, M., Honma, I., Zhou, H., 2006. Adv. Funct. Mater. 16, 371-376.

Luo, X., Morrin, A., Killard, A.J., Smyth, M.R., 2006. Electroanalysis 18, 319-326.

Lv, M., Wei, M., Rong, F., Terashima, C., Fujishima, A., Gu, Z.-Z., 2010. Electroanalysis 22, 199-203.

Moldoveanu, S.C., Kiser, M., 2007. J. Chromatogr. A 1141, 90-97.

Ozoner, S.K., Yalvac, M., Erhan, E., 2010. Curr. Appl. Phys. 10, 323-328.

Sarma, A.K., Vatsyayan, P., Goswami, P., Minteer, S.D., 2009. Biosens. Bioelectron. 24, 2313-2322.

Singh, S., Jain, D.V.S., Singla, M.L., 2013. Sens. Actuators B 182, 161-169.

Song, W., Li, D.-W., Li, Y.-T., Li, Y., Long, Y.-T., 2011. Biosens. Bioelectron. 26, 3181-3186.

Vicentini, F.C., Janegitz, B.C., Brett, C.M.A., Fatibello-Filho, O., 2013. Sens. Actuators B 188, 1101-1108.

Figure captions

Fig. 1. (a) Schematic diagram showing the LbL process on a AuNP deposited SPCE. (b) SEM and (c) AFM images alongside the height profile of a AuNC-(PSS-AuNC)$_2$-MPA-AuNP-SPCE. The scanned electrode area is 3 μm × 3 μm. (d) Representative cyclic voltammograms for different concentrations of catechol using a Tyr-AuNC-(PSS-AuNC)$_2$-MPA-AuNP-SPCE. In (d), (i) is no catechol present, and in the presence of (ii) 5.0, (iii) 30 and (iv) 80 μM catechol concentrations. Scan rate = 30 mV s^{-1}.

Fig. 2. A series of square wave voltammograms for catechol sensing using three different biosensor configurations; (a) Tyr-AuNC-(PSS-AuNC)$_2$-MPA-AuNP-SPCE, (b) Tyr-AuNP-SPCE and (c) Tyr-CTAB$^+$-(PSS$^-$-CTAB$^+$)$_2$-MPA-AuNP-SPCE. In (a), (i) is the absence of catechol, and in the presence of (ii) 0.05, (iii) 3.0, (iv) 10, (v) 20, (vi) 40, (vii) 60 and (viii) 80 μM catechol. In (b), (i) is the absence of catechol, and in the presence of (ii) 0.8, (iii) 5.0, (iv) 40, (v) 80 and (vi) 120 μM catechol. In (c), (i) is the absence of catechol, and in the presence of (ii) 5.0, (iii) 20, (iv) 40, (v) 60 and (vi) 70 μM catechol. Scan rate = 30 mV s^{-1} (cyclic voltammetry). For SWV, a sweep potential between +0.3 V to -0.4 V with a step potential of 10 mV, an amplitude of 50 mV and a frequency of 15 Hz were used.

Fig. 3. Plots of SWV peak currents versus various concentrations of catechol using (a) Tyr-AuNC-(PSS-AuNC)$_2$-MPA-AuNP-SPCE, (b) Tyr-AuNP-SPCE and (c) Tyr-CTAB$^+$-(PSS$^-$-CTAB$^+$)$_2$-MPA-AuNP-SPCE. The catechol concentrations were varied in (a) 0.1 to 80 µM, (b) 0.8 to 120 µM, and (c) 2.0 to 70 µM. Inset shows the linear response for catechol concentrations from 10 to 100 nM using the (a) biosensor design.

Revised Figure 1

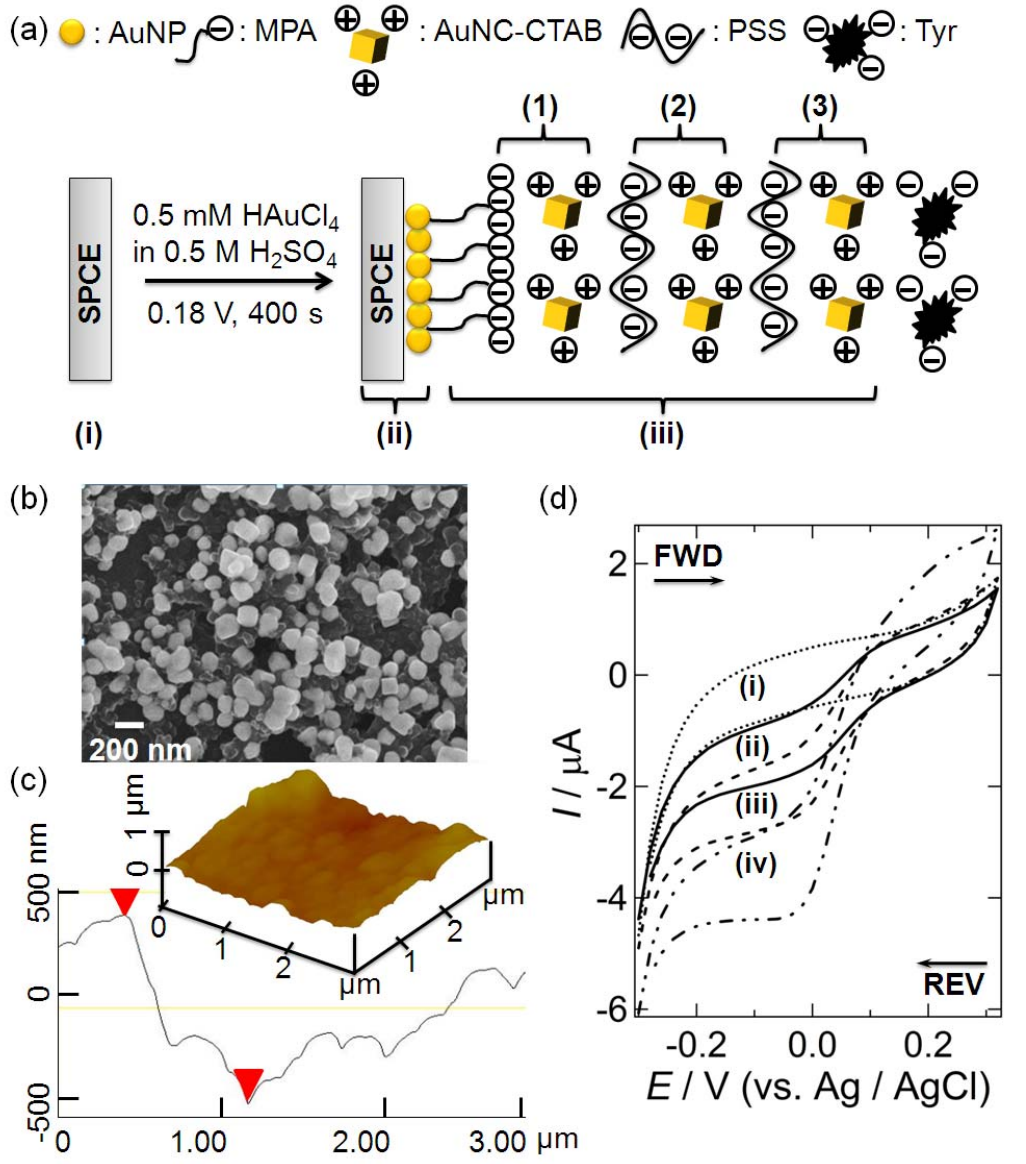

Figure 2

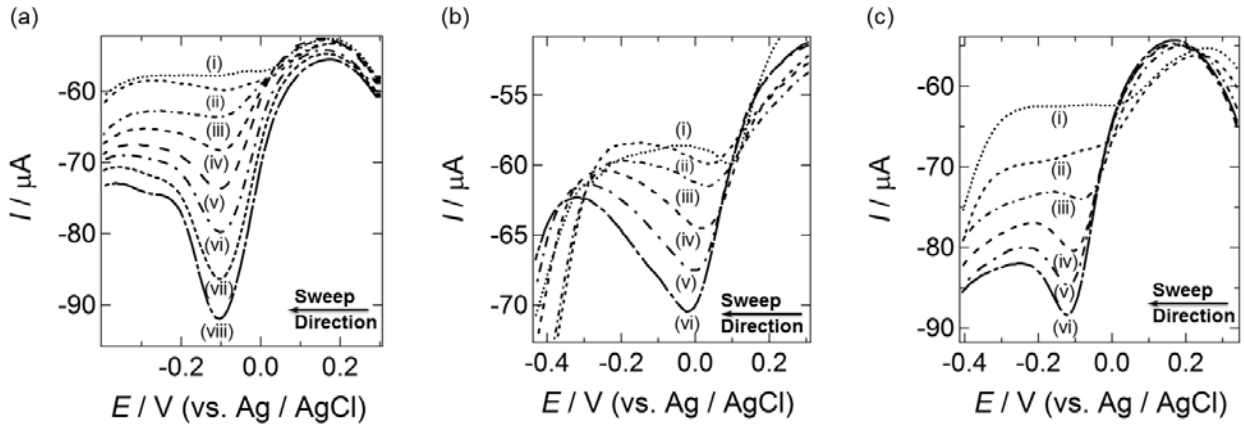

Revised Figure 3

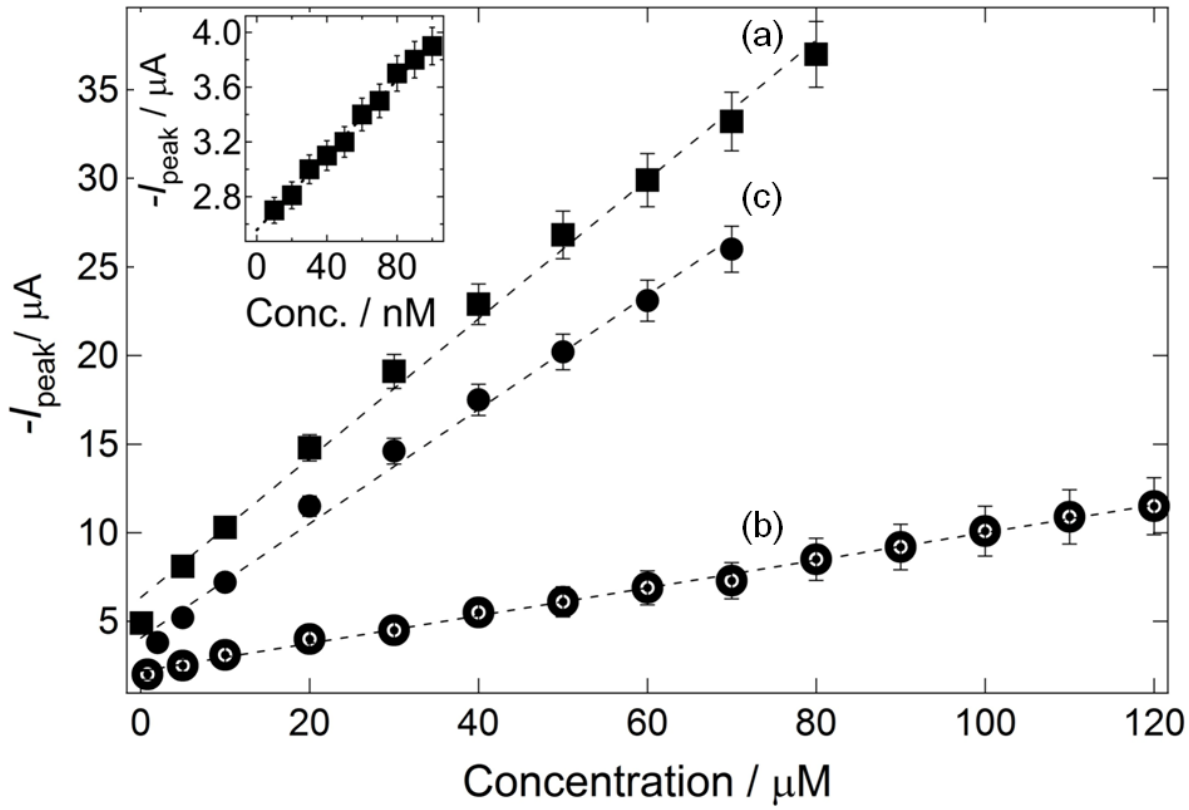

Highlights:

- A novel gold nanocube (AuNC) enhanced amperometric biosensor for catechol molecules
- Layer-by-layer assembly of AuNC's, polyelectrolytes and tyrosinase on an electrode
- Highly reproducible nanostructured biosensors offering cheap and easy configuration
- Excellent sensitivity and detection limit enhanced by AuNC incorporation
- Direct analysis of catechol in tea samples to highlight sensor applicability